

1q12 chromosome translocations form aberrant heterochromatic foci associated with changes in nuclear architecture and gene expression in B cell lymphoma

Alexandra Fournier^{1,2,†}, Anne McLeer-Florin^{1,2,3,†}, Christine Lefebvre^{1,2,3}, Samuel Duley^{1,2}, Leila Barki^{1,2}, Juliana Ribeyron^{1,2}, Alboukadel Kassambara^{1,2}, Sieme Hamaidia^{1,2}, Aurélie Granjon^{1,2}, Rémy Gressin^{1,2,4}, Alicia Lajmanovich^{1,2,5}, Thierry Bonnefoix^{1,2,5}, Stéphanie Chauvelier^{1,2}, Alexandra Debernardi^{1,2}, Sophie Rousseaux^{1,2}, Florence de Fraipont^{1,2,6}, Martin Figeac⁷, Jean-Pierre Kerckaert⁸, John De Vos⁹, Yves Usson¹⁰, Katia Delaval¹¹, Alexei Grichine^{1,2}, Claire Vourc'h^{1,2}, Saadi Khochbin^{1,2}, Robert Feil¹¹, Dominique Leroux^{1,2,3}, Mary B. Callanan^{1,2,3*}

Keywords: B cell lymphoma; *GMCL1*; heterochromatic foci; nuclear architecture; 1q12 pericentric heterochromatin

DOI 10.1002/emmm.201000067

Received September 18, 2009
Revised February 19, 2010
Accepted February 24, 2010

See related article by Dias-Santagata D *et al*
DOI 10.1002/emmm.201000070.

Epigenetic perturbations are increasingly described in cancer cells where they are thought to contribute to deregulated gene expression and genome instability. Here, we report the first evidence that a distinct category of chromosomal translocations observed in human tumours—those targeting 1q12 satellite DNA—can directly mediate such perturbations by promoting the formation of aberrant heterochromatic foci (aHCF). By detailed investigations of a 1q12 translocation to chromosome 2p, in a case of human B cell lymphoma, aberrant aHCF were shown to be localized to the nuclear periphery and to arise as a consequence of long range ‘pairing’ between the translocated 1q12 and chromosome 2 centromeric regions. Remarkably, adjacent 2p sequences showed increased levels of repressive histone modifications, including H4K20me3 and H3K9me3, and were bound by HP1. aHCF were associated to aberrant spatial localization and deregulated expression of a novel 2p gene (*GMCL1*) that was found to have prognostic impact in diffuse large B cell lymphoma. Thus constitutive heterochromatin rearrangements can contribute to tumourigenesis by perturbing gene expression via long range epigenetic mechanisms.

(1) INSERM U823, Institut Albert Bonniot, Grenoble, France.

(2) Université Joseph Fourier-Grenoble I, Institut Albert Bonniot, UMR-S823, Grenoble, France.

(3) Onco-Hematology Genetics Unit, Plateforme Hospitalière de Génétique Moléculaire des Tumeurs, Department of Hematology, Onco-Genetics and Immunology, Pôle de Biologie, CHU de Grenoble, France.

(4) Pôle de Cancérologie et d'Hématologie, CHU de Grenoble, Grenoble, France.

(5) Pôle Recherche, CHU de Grenoble, Grenoble, France.

(6) UF Cancérologie Biologique et Biothérapies, Pôle de Biologie, CHU Grenoble, Grenoble, France.

(7) Université Lille Nord de France, UDSL, Plate-Forme de Génomique IFR-114, IRCL, Lille, France.

(8) INSERM U837, UDSL, IFR-114 and IRCL, Lille, France.

(9) INSERM U847, Montpellier, France.

(10) Laboratoire TIMC, Equipe RFMQ, CNRS UMR 5525, La Tronche, France.

(11) Institute of Molecular Genetics, CNRS UMR-5535, University of Montpellier II, Montpellier, France.

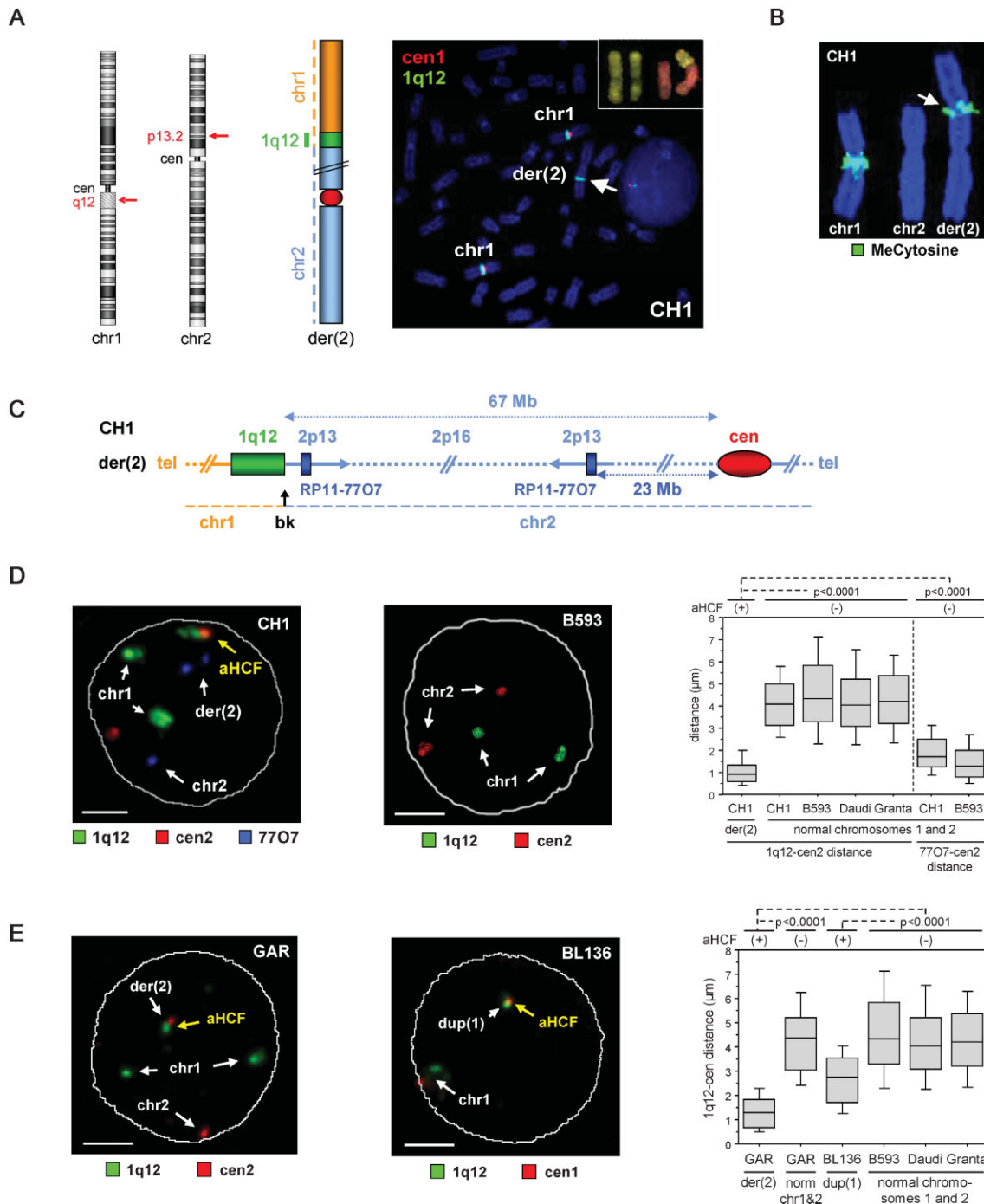
*Corresponding author: Team ‘Oncogenic Pathways in the Haematological Malignancies’ Institut National de la Santé et de la Recherche Médicale (INSERM), Université Joseph Fourier Research Centre, U823, Institut Albert Bonniot, Grenoble F-38706, France. Tel: +33-476549584; Fax: +33-4765499425; E-mail: mary.callanan@ujf-grenoble.fr

†Contributed equally to this work.

INTRODUCTION

Cancer initiation and progression are increasingly recognized as multistep processes that involve the acquisition of both genetic and epigenetic perturbations (Feinberg et al, 2006). In particular, genetic aberrations such as chromosomal translocations encoding oncogenic fusion genes have been intensely studied and have led to groundbreaking advances in the

identification of novel oncogenic signalling pathways and therapeutic targets, as well as serving as important cancer biomarkers (Rabbits, 2009). In addition, we and others have described a novel category of chromosomal aberration that involves constitutive heterochromatin derived from human chromosome 1 (cytogenetic band 1q12; Busson-Le Coniat et al, 1999; Itoyama et al, 2002; Le Baccon et al, 2001). These rearrangements are particularly frequent in haematopoietic and



solid tumours thereby arguing in favour of a role for constitutive heterochromatin-linked oncogenic mechanisms in these disorders (Fournier et al, 2007). Although an attractive hypothesis no study to date has addressed this question.

Constitutive heterochromatin is a specialized compartment within chromatin that is found primarily at centromeres, telomeres and the pericentric regions of certain chromosomes. It is composed of gene-poor, repetitive DNA sequence (alpha satellite, satellite II and III) that shows distinct epigenetic features, *i.e.* late-replication, high levels of DNA methylation and 'repressive' histone modifications such as histone H4 lysine 20 (H4K20me3) and histone H3 lysine 9 (H3K9me3) trimethylation that mediate heterochromatin formation and recruitment of maintenance proteins such as HP1 (Grewal & Jia, 2007). Evidence also exists for an RNA component in heterochromatin formation (Bernstein and Allis, 2005; Grewal & Jia, 2007).

Apart from its role in the control of genomic stability, constitutive heterochromatin influences the regulation of gene expression in numerous species through a mechanism known as 'position effect'. This phenomenon results from a little-understood process of heterochromatin '*cis*' or '*trans*' spreading into adjacent euchromatin and which induces gene repression (Grewal & Jia, 2007). This mechanism also appears to operate in mammalian cells. For example, during lymphoid development, stable transcriptional repression of certain lymphoid-specific genes is tightly correlated to their association with constitutive heterochromatin and acquisition of repressive histone modifications (Brown et al, 1997, 1999; Grogan et al, 2001; Su et al, 2004). It is also emerging that spatial positioning of genes with respect to constitutive heterochromatin and to the

nuclear periphery constitutes additional complex epigenetic mechanisms that contribute to 'positional' gene regulation during development and cellular differentiation (Finlan et al, 2008; Kumaran & Spector, 2008; Reddy et al, 2008). Whether such processes are deregulated in human tumours has not been investigated in any detail.

No study has investigated the potential pathological consequences of the presence of altered 1q12 constitutive heterochromatin on gene expression and on chromatin organization in either haematological or solid tumours. In this context, we set out to perform the first detailed genetic and epigenetic characterization of 1q12 rearrangements in a human tumour by using B cell lymphoma as a study model.

RESULTS AND DISCUSSION

Translocations targeting 1q12 satellite DNA provoke long-range intrachromosomal interactions that lead to the formation of aberrant heterochromatic foci (aHCF) in human B-cell lymphoma

As a first step towards investigating the genetic and epigenetic consequences of constitutive 1q12 heterochromatin rearrangements in lymphoid malignancies, we selected as a model system, a human B lymphoma line, CH1, that harbours a novel t(1;2)(q12;p13) translocation (Barki-Celli et al, 2005). This unbalanced translocation involves juxtapositioning of a large block of 1q12 satellite II-rich sequence to the chromosome 2p arm (Fig 1A, arrow and Fig S1 of the Supporting Information). In keeping with reported cytogenetic observations of similar

Figure 1. Formation of aHCF in lymphoma B cells presenting rearrangements that target 1q12 constitutive heterochromatin.

- (A) Dual colour FISH showing the t(1;2) translocation in CH1 cells. Three 1q12 FISH signals (green) are visible, one of which is translocated to the short arm of the der(2) chromosome (white arrow). Red FISH signals correspond to chromosome 1 centromeres. Upper right inset shows M-FISH on normal chromosomes 1 (yellow) and 2 (pink) and on the der(2) chromosome (yellow and pink). Cartoons indicating t(1;2) breakpoints on chromosomes 1 and 2 (red arrows), as well as the der(2) chromosome (left panel).
- (B) Immunodetection of methylated DNA on mitotic chromosomes by an anti-MethylCytosine antibody, in CH1 cells. Note intense labelling at the juxtacentromeric 1q12 band on normal chromosome 1 and at the 1q12/2p breakpoint region on the der(2) chromosome (white arrow).
- (C) Physical map of the der(2) breakpoint region showing the orientation of the duplicated 2p region with respect to the 1q12/2p breakpoint (black arrow). The 1q12 proximal 2p region is in the reverse order, compared to the germline region on the same chromosome, as indicated on the map (facing horizontal thick blue arrows). Regions analysed by FISH (1q12 heterochromatin, chromosome 2 centromere and RP11-7707 (2p BAC) are indicated on the map. The t(1;2) breakpoint (bk) is indicated by a black arrow.
- (D) 3D FISH with 1q12 (green), chromosome 2 centromere (red) and RP11-7707 2p BAC (blue)-specific probes, detects formation of an aberrant constitutive heterochromatic structure ('aHCF', yellow arrow) in CH1 lymphoma B cells (left panel) but not in control lymphoma B cells without 1q12 anomalies (right panel, and Fig S2B of the Supporting Information). The images were obtained by the maximum z-projection of red and green stacks after deconvolution. DAPI staining was outlined in the equatorial plane of the nucleus. Box-plots (far right panel) showing nuclear distance distributions (in μm) between 1q12 and chromosome 2 centromere regions on the der(2) chromosome (on which they are separated by 67 Mb) and on the normal chromosomes 1 and 2, in lymphoma B cells presenting aHCF (CH1) compared to control lymphoma B cells (B593, Daudi, Granta 519) (no heterochromatic foci, 2 normal copies of chromosome 2), and compared to nuclear distance distributions (in μm) between RP11-7707 2p BAC and chromosome 2 centromere (separated by 23 Mb), in CH1 and B593 cells; Kolmogorov-Smirnov test, $p < 0.0001$.
- (E) 3D FISH with 1q12 (green) and chromosome 2 (GAR, left panel) or 1 (BL136, middle panel) centromere-specific probes (red), detects formation of aHCF (yellow arrow) in GAR primary lymphoma B cells and in the Burkitt lymphoma cell line BL136 (left and middle panels, respectively). The image was obtained as described in (D). Box-plots (far right panel) showing nuclear distance distributions (in μm) between 1q12 and chromosome 2 or 1 centromere regions on the der(2) or dup(1) chromosomes and on the normal chromosomes 1 and 2, in lymphoma B cells presenting aHCF (GAR, BL136) compared to B593, Daudi and Granta lymphoma B cells (no heterochromatic foci, 2 normal copies of chromosome 2), as indicated; Kolmogorov-Smirnov test, $p < 0.0001$. The number of nuclei analysed for distances measurements was 63 in CH1, 57 in GAR, 63 in BL136, 89 in B593, 101 in Daudi and 85 in Granta; 62 (RP11-7707) in CH1 and 69 (RP11-7707) in B593. der(2), derivative of chromosome 2; dup(1), duplicated chromosome 1; aHCF, aberrant heterochromatic foci. Scale bar: 2 μm .

rearrangements in other tumours (Fournier et al, 2007) #2330), karyotyping (not shown) and FISH, in our lymphoma case, showed that the translocated 1q12 region remained cytologically condensed (Fig 1A, right panel), thus suggesting that it maintained a heterochromatic conformation. In agreement with this, immunofluorescence detection of methylated DNA on mitotic chromosomes revealed dense methylation on the normal and the translocated 1q12 region but not on the normal chromosome 2 (Fig 1B). Furthermore, immuno-FISH revealed clear co-localization of 1q12 FISH signals—including the translocated 1q12 region—with heterochromatin foci enriched in H3K9me3 (Fig S2A of the Supporting Information). This confirmed that translocated 1q12 retained epigenetic hallmarks of constitutive heterochromatin.

The 1q12/2p junction in CH1 cells was then mapped by high resolution array-CGH and FISH (Fig 1C and Fig S1 of the Supporting Information). This pinpointed the 1q12/2p breakpoint to chromosome band 2p13 in addition to identifying a 33.5 Mb ‘mirror image’ duplication, at 2p13, on the der(2) chromosome (Fig 1C and Fig S1 of the Supporting Information). This genetic complexity was not entirely unexpected, since duplication events are quite frequent at the acceptor sites for 1q12 heterochromatin translocations in lymphoma and myeloma (Sawyer et al, 1998, 2005).

The spatial proximity and nuclear organization of the 1q12 and centromere 2 constitutive heterochromatin domains were then examined by FISH in 3D-preserved, CH1 lymphoma B cell nuclei, compared to control lymphoma B cells that do not present 1q12 anomalies (Fig 1D). The 1q12 and chromosome 2 centromeric regions, on the der(2) in CH1 cells are separated by 67 Mb in linear genomic terms (Fig 1C) and thus FISH signals were expected to be well resolved in CH1 interphase nuclei. Quite strikingly, the opposite was the case; the 1q12 and centromere 2 FISH signals on the der(2) chromosome appeared to be fused and to form abnormal heterochromatic structures that we have termed aberrant heterochromatic foci (‘aHCF’) (Fig 1D). Detailed distance measurements in these cells further confirmed these findings; the 1q12 and centromere 2 interprobe FISH distances on the der(2) in CH1 nuclei were significantly shorter than expected when compared to interprobe distances measured at a control 2p region [flanked by the BAC probe, RP11-7707, (blue signals) and the chromosome 2 centromere (red signals); 23Mb, Fig 1C and D], in either CH1 or B593 lymphoma B cells (Fig 1D, far right panel, Kolmogorov–Smirnov test, $p < 0.0001$, and Table S1 of the Supporting Information). Importantly, fusion of 1q12 and centromere 2 heterochromatic regions was not observed in control lymphoma B cells, without 1q12 anomalies (Fig 1D middle and far right panels and Fig S2B of the Supporting Information; B593, Daudi and Granta 519 lymphoma B cells). Taken together, this was the first indication that 1q12 heterochromatin rearrangements are associated to long-range intrachromosomal interactions that drive the formation of aHCF structures in lymphoma B cells (Fig 1D, Fig S3 of the Supporting Information). Furthermore, aHCF in CH1 lymphoma B cells were observed in unsynchronized cells and were found to be stably propagated over cell division suggesting that these structures are maintained during a

considerable part of interphase and that they are reassembled after cell division.

We next assessed whether the formation of such aHCF might be a recurrent feature of 1q12 rearrangements in tumour B cells. Remarkably, aHCF were observed in two additional cases of B-cell lymphoma presenting 1q12 anomalies; primary lymphoma B-cells (GAR) from a diffuse large B cell lymphoma patient that presented a der(2)t(1;2)(q12;q37) and in the Burkitt lymphoma cell line, BL136, that showed a dup(1)(q12;q42) (Barki-Celli, 2005, #2031) (Fig 1E, left and middle panels, respectively). In both cases, distance measurements between 1q12 (green) and chromosome 1 (BL136) or 2 (GAR) centromere (red) FISH signals again revealed dramatically increased spatial proximity of these two heterochromatic domains (Fig 1E, far right panel; Kolmogorov–Smirnov test, $p < 0.0001$). These heterochromatic structures are striking and have not been previously reported for any chromosomal rearrangement in a human tumour. Taken together, this is strong evidence that 1q12 pericentric heterochromatin rearrangements constitute a new class of chromosomal aberrations that perturb nuclear architecture through long range intrachromosomal interactions and the formation of aHCF.

Aberrant heterochromatic foci are associated to variable enrichment of adjacent 2p sequences in H4K20me3, H3K9me3 and HP1

We next investigated the potential consequences of the presence of aHCF on chromatin organization and function in lymphoma B cells. For this, we took advantage of the CH1 lymphoma B cells to perform detailed ChIP to ‘repressive’ heterochromatin marks (H4K20me3, H3K9me3 and HP1 α , β and γ) on 2p sequences that were brought into close physical or spatial proximity to aberrant heterochromatin foci. High resolution array-CGH and FISH-based mapping of the 1q12/2p breakpoint region had localized the 1q12/2p breakpoint within intron 6 of the *EXOC6B* gene (coordinate 72,760,219 in chromosome band 2p13, Fig 2A and Fig S1 of the Supporting Information). Thus, in genetic terms, the t(1;2) observed in CH1 cells resulted in juxtapositioning of intron 6, of a duplicated copy of the *EXOC6B* gene, in the reverse orientation, to 1q12 constitutive heterochromatin (Fig 2A). Site-specific, quantitative ChIP analyses to the aforementioned heterochromatin ‘marks’ were performed at the 3’ region of the *EXOC6B* gene, the proximal promoter regions and exons 1 and 2, of the *CYP26B1* and *ZNF638* genes, respectively, and two intergenic sequences (ig1 and ig2, both localized between *CYP26B1* and *ZNF638*) (Fig 2A). ChIP which was carried out on native (histone modifications) or fixed chromatin (HP1) was also performed to satellite II repeats (enriched at 1q12) and *GAPDH*, as a control euchromatic region (Fig 2B and C) (primer details, Table SIII of the Supporting Information).

Q-ChIP in the lymphoma B cells showing aberrant heterochromatin foci (CH1), compared to control cells (B593), revealed increased precipitation of H3K9me3 and/or H4K20me3 over all 2p sequences tested, although precipitation levels were seen to be variable (Fig 2B). This is in agreement with findings in two classical heterochromatin ‘spreading’ models (*Drosophila white* locus and X-autosome translocations) which indicate that *de*

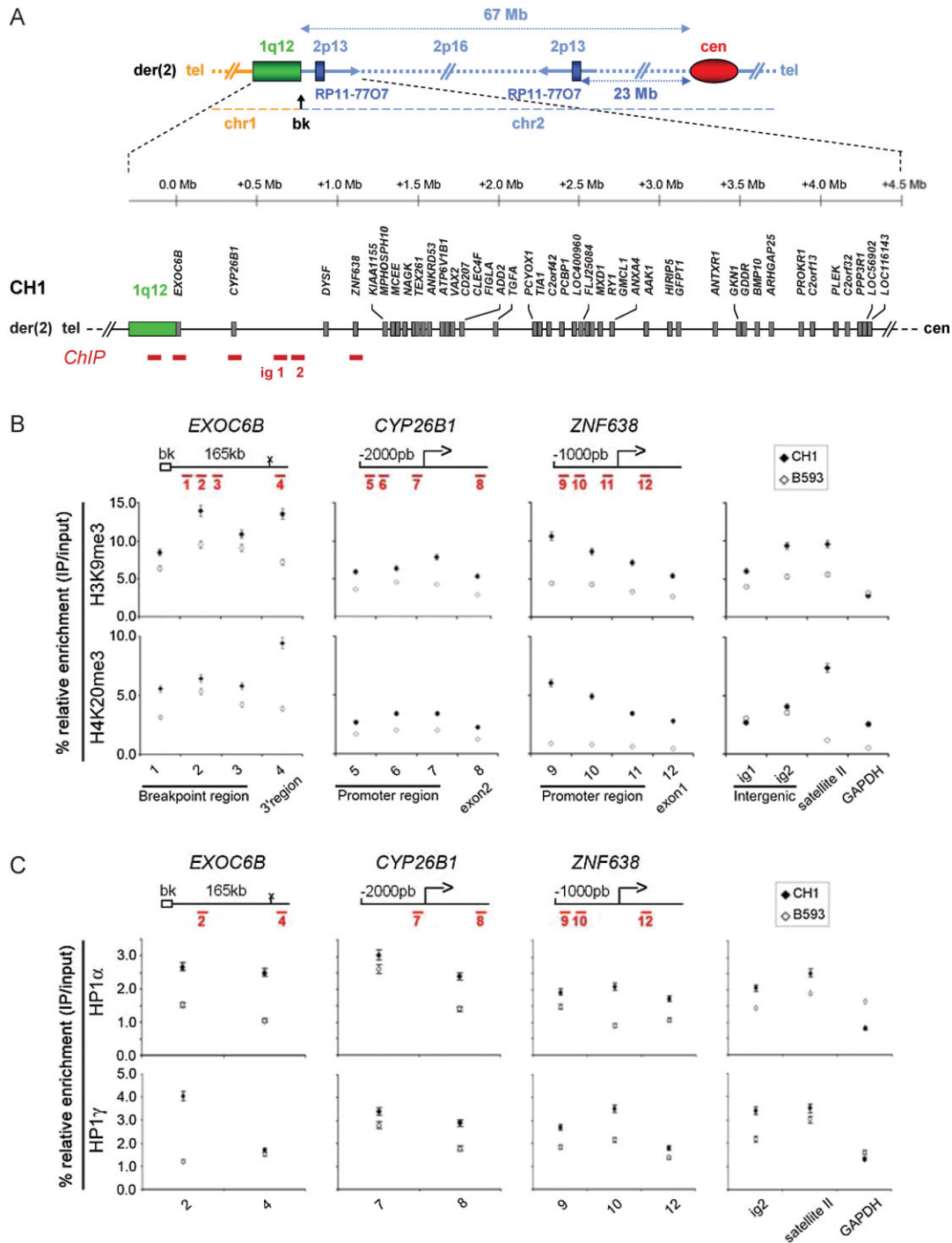


Figure 2. Long range enrichment in repressive heterochromatin ‘marks’ at 2p sequences in close physical or spatial proximity to aberrant 1q12/ chromosome 2 heterochromatic foci.

- (A) Physical map of the der(2) breakpoint region (top panel as in Fig 1C), showing the genomic positions of 2p genes with respect to the 1q12/2p breakpoint (black arrow top panel; bottom panel, set to 0.0 Mb), in a 5 Mb region. Regions analysed by ChIP in (B) and (C) are indicated underneath the map (horizontal red bars).
- (B) ChIP for histone modifications, as indicated, followed by Q-PCR analysis for enrichment levels, at the indicated 2p regions. Location of 2p sequences analysed by ChIP are indicated by a red bar on the gene maps shown above the respective ChIP panels. Primer pairs are numbered (Table SIII of the Supporting Information).
- (C) HP1 Q-ChIP on fixed chromatin at selected sites from (B). HP1 isoforms studied are indicated on the left of the Q-ChIP histograms. ChIP analysis show HP1 α and/or HP1 γ enrichment at most of the selected sequences analysed. The curves show the mean of at least two independent experiments with error bars indicating the standard deviation. bk, breakpoint.

*nov*o formed heterochromatin may be less stable than naturally occurring constitutive heterochromatin (Popova et al, 2006; Vogel et al, 2009). Of note, the profiles observed differed from those seen for H3K27me₃, a histone modification associated to facultative heterochromatin (Fig S4A of the Supporting Information; no obvious increase in precipitation levels).

We next probed for HP1 binding at the same sites. For this, cross-linked ChIP to all 3 HP1 isoforms (α , β and γ) was performed in the lymphoma B cells showing aHCF (CH1) compared to control cells (B593) (Fig 2C, HP1 α and γ ; Fig S4B of the Supporting Information, HP1 β). All of the examined sequences including the *CYP26B1* gene promoter, showed marked enrichment of both HP1 α and γ (Fig 2C). HP1 β enrichment was less pronounced or equivalent in CH1 compared to B593 cells (Fig S4B of the Supporting Information). As observed for histone modifications,

this was not due to global increases in HP1 levels which by Western blotting were unchanged (data not shown). Of note, DNA methylation analyses did not reveal aberrant methylation, at least at the *CYP26B1* and *ZNF638* genes (data not shown).

We also remarked that precipitation levels for both H3K9me₃ and H4K20me₃ were higher in satellite II sequence in the lymphoma B cells with aberrant heterochromatin foci (CH1), compared to the control cells (B593). The reason for this was not investigated further but may reflect abnormal HMTase activity, as a consequence of aHCF, at these sites (Krouwels et al, 2005; Souza et al, 2009). Taken together, these ChIP experiments provide evidence that aberrant heterochromatin foci are associated to increased HP1 deposition at adjacent euchromatin, probably reflecting abnormal levels of H4K20me₃ and/or H3K9me₃, at the same sites.

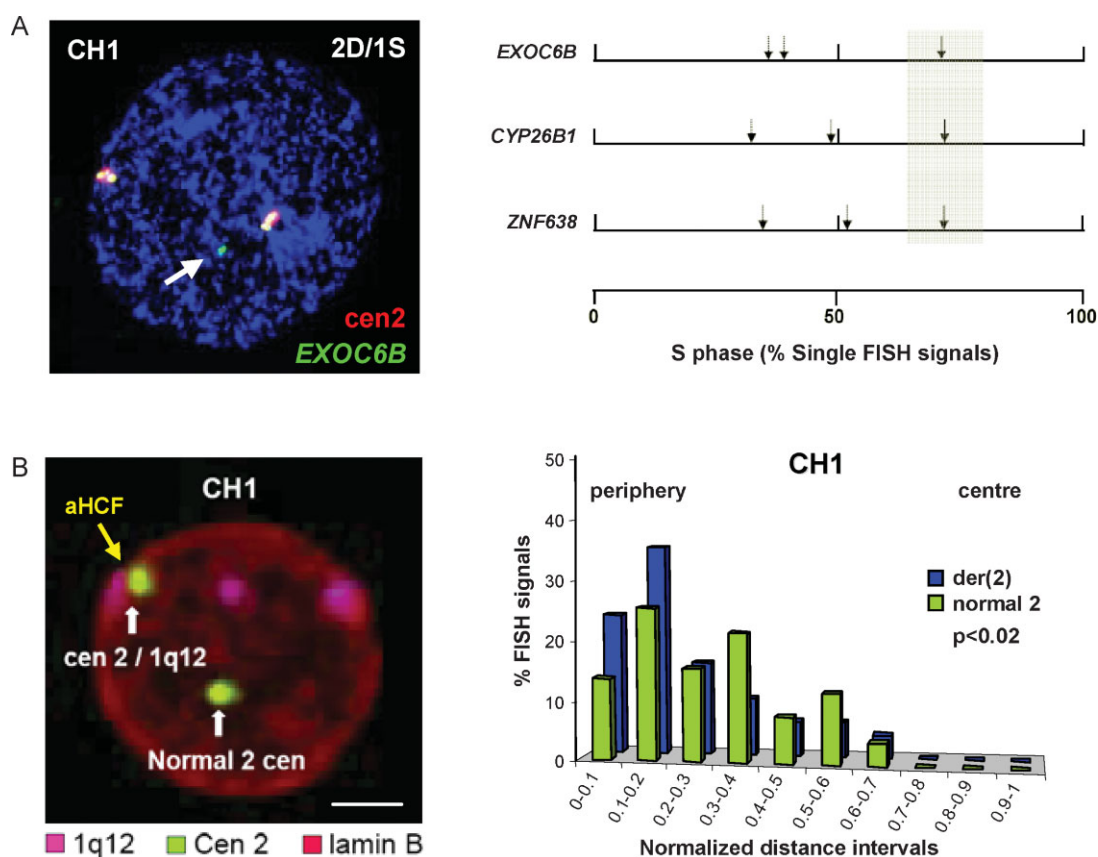


Figure 3. Delayed replication at the 1q12/2p13 breakpoint and abnormal repositioning of the der(2) chromosome to the nuclear periphery in CH1 lymphoma B cells.

- (A) Replication timing. Left panel: a representative FISH picture showing an un-replicated (single, S) FISH signal for the breakpoint proximal copy of the *EXOC6B* gene (green, white arrow), two replicated (double, D) FISH signals for the breakpoint distal and normal *EXOC6B* copies and unreplicated FISH signals (red) for the chromosome 2 centromere. Right panel: per cent single (un-replicated) FISH signals for the breakpoint proximal copies of the *EXOC6B*, *CYP26B1* and *ZNF638* breakpoint proximal copies (far right arrow; grey zone) compared to the more distal copies (middle vertical arrows) on the der(2) and compared to the normal chromosome 2 (far left vertical arrows). FISH in 200 BrdU-labelled nuclei.
- (B) 3D-immuno-FISH. Left panel: a representative nucleus (confocal stack) compiled from single equatorial optical sections. The nuclear membrane is detected by an anti-lamin B antibody (red), 1q12 domains (pink) and chromosome 2 centromeres (green) are detected by specific probes. Right panel: analysis of radial nuclear distributions of 1q12 domains for both normal (green histograms) and derivative chromosome 2 (blue histograms). aHCF, aberrant heterochromatic foci. Scale bar: 2 μ m.

Aberrant heterochromatic foci in CH1 cells are associated to delayed replication of 1q12/2p13 breakpoint proximal genes and abnormal repositioning of the der(2) chromosome to the nuclear periphery

Replication timing is a mitotically stable yet cell type-specific feature of chromosomes that reflects higher-order organization of the genome (Hiratani & Gilbert, 2009). We reasoned that the observed increases in precipitation levels of 2p breakpoint sequences, in 'repressive' chromatin marks (H3K9me3, H4K20me3 and HP1) might be associated to altered replication (delayed) of the affected sequences, compared to the normal chromosome 2 in CH1 and control lymphoma B cells (B593). This was indeed the case; the percentage of single (un-replicated) FISH signals for each of the three gene copies (*EXOC6B*, *CYP26B1* and *ZNF638*) located immediately adjacent to the breakpoint site (proximal copies), was significantly higher than that observed for the two other gene copies either on the der(2) or normal 2 chromosomes [see Fig 3A; % un-replicated signals for the proximal gene copies (shaded in grey); *EXOC6B* (66.5%), *CYP26B1* (67.2%) and *ZNF638* (63.7%)]. Some asynchronous replication between the 'breakpoint distal' and normal 2p gene copies was also seen in CH1 lymphoma B cells. However, this was also observed in the control lymphoma B cells (B593) [fully replicated signals for the 3 genes were observed in 51.5% (*EXOC6B*), 35% (*CYP26B1*) and 28% (*ZNF638*), of cells respectively]. In the remaining B593 cells, the three genes were either unreplicated (<15% S phase nuclei) or asynchronously replicated (data not shown).

We next assessed whether the formation of such aHCF and correlated replication delays might be associated to perturbed nuclear organization, as has been described in a *Drosophila* position effect model (Dernburg et al, 1996). Remarkably, 3D immuno-FISH in the lymphoma B cells presenting the aberrant heterochromatin foci (CH1 tumour B cells) revealed abnormal relocalization of the der(2) chromosome to the nuclear periphery, compared to the normal chromosome 2, which maintains a more central position (Fig 3B).

Aberrant heterochromatic foci are associated to deregulation of the germ cell less 1 (*GMCL1*) gene in CH1 lymphoma B cells

The formation of aHCF, coupled to abnormal enrichment of adjacent 2p sequences in repressive heterochromatin marks (H4K20me3, H3K9me3 and HP1), delayed replication and repositioning of the rearranged chromosome 2 to the nuclear periphery, could be associated to altered gene expression of at least those genes brought into close proximity to heterochromatin (Grewal and Jia, 2007; Hiratani and Gilbert, 2009; Takizawa et al, 2008). To assess this question, global gene expression profiling was performed in the lymphoma B cells presenting the aberrant heterochromatin foci (CH1), treated or not with the histone deacetylase inhibitor, trichostatin A (TSA), by using U133 2.0 Affymetrix gene chip arrays (GSE20666). For the reasons outlined above, we focused our differential gene expression analysis on a 5 Mb 2p interval (including the 1 Mb 2p region analysed by ChIP) likely to be either physically or spatially positioned close to aberrant heterochromatin foci (Fig 4A). Briefly, as a first step, we took advantage of Affymetrix U133 2.0 and Agilent 244 k array

CGH profiling, from the aHCF presenting case, CH1, to perform 'moving average' analysis, in 500 kb-sized windows in the 5 Mb 2p breakpoint region, compared to regions of equal size and copy number, elsewhere in the CH1 genome (a total of 4833 probes). This analysis pinpointed a 500 kb window containing five genes (*GFPT1*, *HIRIP5*, *AAK1*, *ANXA4*, *GMCL1*) that were deregulated with a *p*-value very close to significance ($p = 0.06$) (Fig 4A). This locus was thus a strong candidate for specific perturbation as a consequence of 1q12 satellite II DNA translocation to 2p in CH1 cells. Among these genes, we focussed on those that were identified by microarray analysis as sensitive to TSA treatment, because these genes would be good candidates to epigenetic deregulation due to aHCF. One gene, *GMCL1*, showed significant differential expression (fold change >2) after TSA treatment (data not shown). This result was confirmed by RT-Q-PCR on CH1 cells treated or not with TSA, 5-aza-2'-deoxycytidine, or TSA + 5-aza-2'-deoxycytidine (Fig 4B, left panel). TSA treatment alone induced a >3-fold increased expression of *GMCL1* in CH1 cells (Fig 4B, left panel, $p < 0.05$). Of note, 5-aza-2'-deoxycytidine had no effect on *GMCL1* expression (Fig 4B, left panel), which was not totally unexpected since this gene promoter is not methylated (data not shown). Furthermore, *GMCL1* mRNA was significantly underexpressed in CH1 cells compared to three lymphoma B cell lines (pooled) and three normal controls (two peripheral blood B cell samples and 1 tonsil B cell sample, pooled) ($p < 0.05$) (Fig 4B, right panel.) We next checked nuclear organization (3D FISH) and heterochromatin marks (ChIP) on the *GMCL1* promoter region. 3D-FISH showed abnormal spatial proximity of the breakpoint proximal copy of the *GMCL1* gene to aHCF [Fig 4C, $p < 0.0001$ by the Kruskal-Wallis test (KW)]. ChIP analysis showed homogeneously high precipitation levels for H4K20me3 and HP1 gamma binding to the *GMCL1* promoter region (Fig 4D). Taken together, these data point to *GMCL1* as a bonafide target for deregulation by 1q12 translocation/aHCF formation, in CH1 lymphoma B cells.

GMCL1 expression levels are correlated to overall survival in diffuse large B cell lymphoma (DLBCL)

GMCL1 encodes a protein that has been implicated in the control of the MDM2-P53 axis and has thus been proposed as a candidate tumour suppressor gene (Masuhara et al, 2003). It was thus of interest to check its expression levels in normal B cells and in B cell lymphoma. Analysis of gene expression data from the Lymphoma/Leukaemia Molecular Profiling Project (Lenz et al, 2008) showed robust expression in peripheral blood B cells and germinal centre centrocytes and centroblasts (Fig 5A). Expression was also observed in DLBCL and levels were comparable between the two molecular subtypes of this disorder (Alizadeh et al, 2000) (Fig 5A, compare activated B cell like 'ABC' to Germinal Centre B cell type 'GCB'). We next determined whether a correlation existed between survival of patients with DLBCL and expression levels of *GMCL1* in the same data set. Strikingly, *GMCL1* mRNA levels showed strong correlation with overall survival in DLBCL (Fig 5B). Furthermore this correlation was maintained in R-CHOP-treated ABC type DLBCL which is a high risk subtype of this disorder (Fig 5C). This suggests that 1q12 satellite DNA rearrangements and associated aHCF have the potential to interfere with the

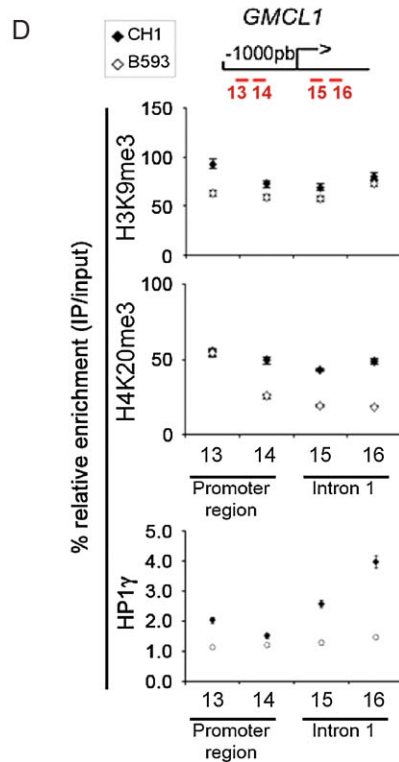
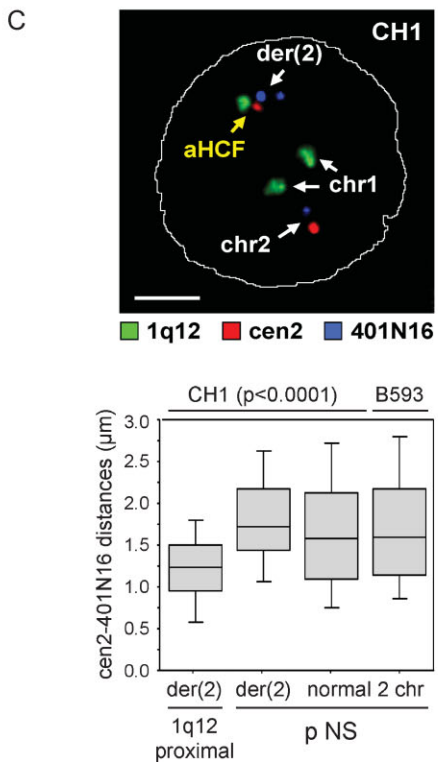
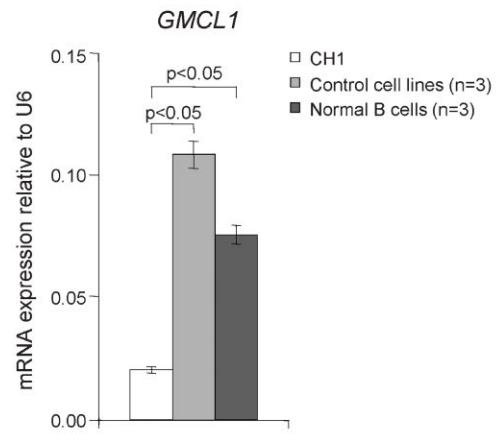
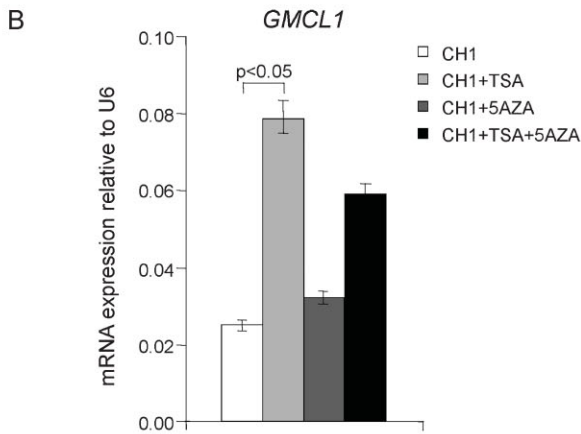
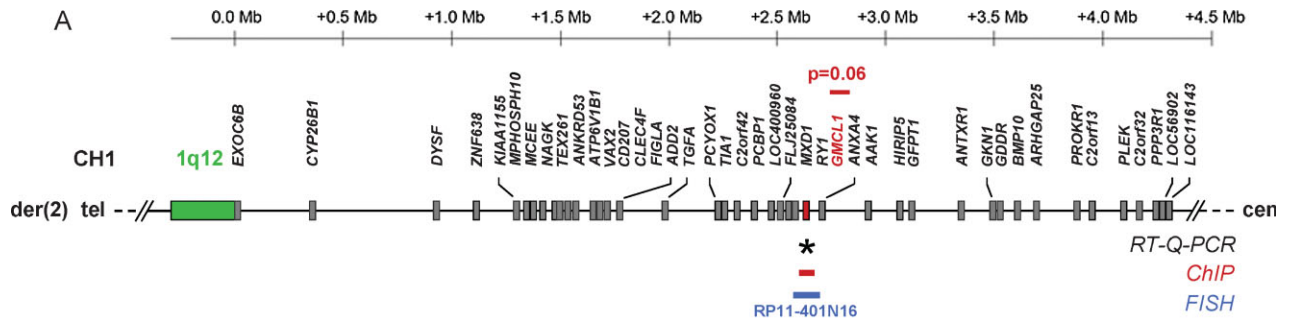


Figure 4. Deregulation of the *GMCL1* locus as a consequence of 1q12 constitutive heterochromatin rearrangement in lymphoma B cells.

- (A) Map of 1q12/2p breakpoint region on der(2) chromosome in CH1 cells, as in Fig 2A; global gene expression profiling was performed in this 5 Mb 2p region located close to the aberrant heterochromatin foci in CH1 lymphoma B cells, treated or not by TSA, by using U133 2.0 Affymetrix gene chip arrays, assessed by GeneSpring software (Agilent). A novel statistical method to identify genes that were significantly deregulated in this 5 Mb 2p region compared to the rest of the genome combined with a test for TSA-sensitivity identified one gene, *GMCL1*. *GMCL1* expression (black star), chromatin status (red bar) and spatial organization (blue bar) were further analysed (B–D).
- (B) RT-Q-PCR analysis of *GMCL1* expression status in CH1 cells treated or not with TSA, 5-aza-2'-deoxycytidine, or TSA + 5-aza-2'-deoxycytidine (left panel), confirmed that TSA treatment induced a >3-fold increased expression (t-test, $p < 0.05$). RT-Q-PCR analysis of *GMCL1* expression status in CH1 cells, a pool of control lymphoma B cells (B593, Daudi and Granta lines; $n = 3$) and a pool of normal B cells (peripheral-blood and tonsil B cells, $n = 3$) (right panel); *GMCL1* is underexpressed in CH1 cells compared to either control cell lines (t-test, $p < 0.05$) or normal B cells (t-test, $p < 0.05$) (right panel). In all cases, expression data was normalized to the U6 control gene. Data represent the mean \pm standard deviation of at least three independent experiments.
- (C) 3D FISH analysis (BAC RP11-401N16) and box-plots showing the distribution of distances from the chromosome 2 centromere to BAC RP11-401N16 (containing *GMCL1*) on the der(2), compared to the normal chromosomes 2, in lymphoma B cell nuclei without (–) or with (+) 1q12 constitutive heterochromatin rearrangements. Distances were measured in 54 CH1 nuclei and 80 B593 nuclei. The images were obtained as described in Fig 1C. Box-plots showing 3D distances between the chromosome 2 centromere and 2p BAC probes, located in either the normal or 1q12/2p breakpoint proximal positions (1q12 proximal) on the der(2) or normal 2 chromosomes, in lymphoma B cells with (+) (CH1 lymphoma B cells) or without (–) (B593, Daudi and Granta lymphoma B cells) aberrant heterochromatin foci. Note the decreased distances between the chromosome 2 centromere and 2p BAC probe signals, at the 1q12/2p breakpoint proximal position in CH1 lymphoma B cells. For simplification, RP11-401N16 is referred to as 401N16, in (C). aHCF are indicated by yellow arrows. Scale bar: 2 μ m.
- (D) Q-PCR analysis of ChIP enrichments calculated as IP/input for the indicated histone modifications and HP1 γ , at the promoter and intron 1 region of *GMCL1*. The curves show the mean of at least two independent experiments with error bars indicating the standard deviation. Primer pairs are indicated in Table SIII of the Supporting Information.

expression and function of novel lymphoma relevant genes. Since these genes are likely to be undergoing epigenetic deregulation, they represent rational targets for therapeutic intervention with epigenetic agents.

In summary, we propose that 1q12 anomalies correspond to a new class of chromosome rearrangements with the power, via novel long range heterochromatin-dependent mechanisms, to profoundly perturb gene organization and function in lymphoma. Our findings are likely to be relevant not only for B cell lymphoma but for additional haematological and solid tumours as well. Indeed, these anomalies are frequently and non-randomly observed in a broad spectrum of human tumours and have been linked to disease progression and poor prognosis, particularly in multiple myeloma (Fournier et al, 2007). Further studies geared to understanding the mechanistic origins of these aHCF as well as their consequences on gene expression and function will be required to fully elucidate their role in cancer initiation and progression.

MATERIALS AND METHODS

Cell culture, cell lines and primary patient cells

Peripheral-blood B lymphocytes were obtained from healthy donors, and tonsil B cells were obtained following routine tonsillectomy, as previously described (Lajmanovich et al, 2009). Primary lymphoma cells were obtained from a patient (GAR) presenting a diffuse large B-cell lymphoma. Normal and tumour B cells were isolated with anti-CD19 immunomagnetic beads at 1 μ g per 1×10^6 cells (CD19 Microbeads, Miltenyi Biotec, Bergisch Gladbach, Germany) as previously described (Lajmanovich et al, 2009). The purity of the sorted B cell populations was assessed by anti-CD3/CD19 antibody double labelling and flow cytometric analysis. Resting B lymphocytes were either used directly or activated *in vitro* using CD40L (Alexis Biochemicals) at

0.5 μ g/ml for 48 h in RPMI complete medium, as previously described (Lajmanovich et al, 2009). The cell lines studied were diffuse large B-cell lymphoma lines CH1 and B593, Burkitt lymphoma lines BL136 and Daudi, and mantle-cell lymphoma line Granta 519. CH1, B593 and BL136 have been described previously (Barki-Celli et al, 2005; Callanan et al, 2000), Daudi and Granta 519 were obtained from ATCC and DSMZ, respectively. Cell lines were checked for absence of mycoplasma contamination (MycAlert mycoplasma detection kit, Lonza, Switzerland). Cell lines and primary B cells were cultivated at 37°C in a humidified 5% CO₂ atmosphere, in RPMI 1640 medium (or DMEM 4.5 g/L medium for Granta 519) supplemented with 10% (or 20% for BL136) heat-inactivated foetal calf serum (Primary B cells, B593 BL136, Daudi, Granta 519) or human AB+ serum (CH1 cells), 100 μ g/ml penicillin–streptomycin, 1.4 mM sodium pyruvate and 1.4 mM non-essential amino acids (Life Technologies, Grand Island, NY, USA). Cases presenting a 1q12 heterochromatin rearrangement are CH1 and BL136 lines, and GAR primary cells. Control cases (without 1q12 anomalies) are B593, Daudi and Granta lines, and normal peripheral-blood and tonsil B cells. Primary, normal or lymphoma B cell samples were obtained following written informed consent. Approval for the study was obtained from the institutional ethics review board of Grenoble university hospital centre.

Immunodetection of Methyl-CpG on mitotic chromosomes

Mitotic chromosome spreads were prepared according to standard techniques (Le Baccon et al, 2001). For DNA methylation analysis by immunodetection, mitotic chromosomes were first irradiated with ultraviolet light in a shallow suspension of 1 \times phosphate buffered saline (1 \times PBS) for 90 min. Following denaturation the slides were immersed in 1% paraformaldehyde for 10 min at 4°C, and then rinsed three times in a modified 1 \times PBS solution (1 \times PBS, 0.3% BSA fraction V, 0.1% Tween-20). Metaphases spreads were then treated

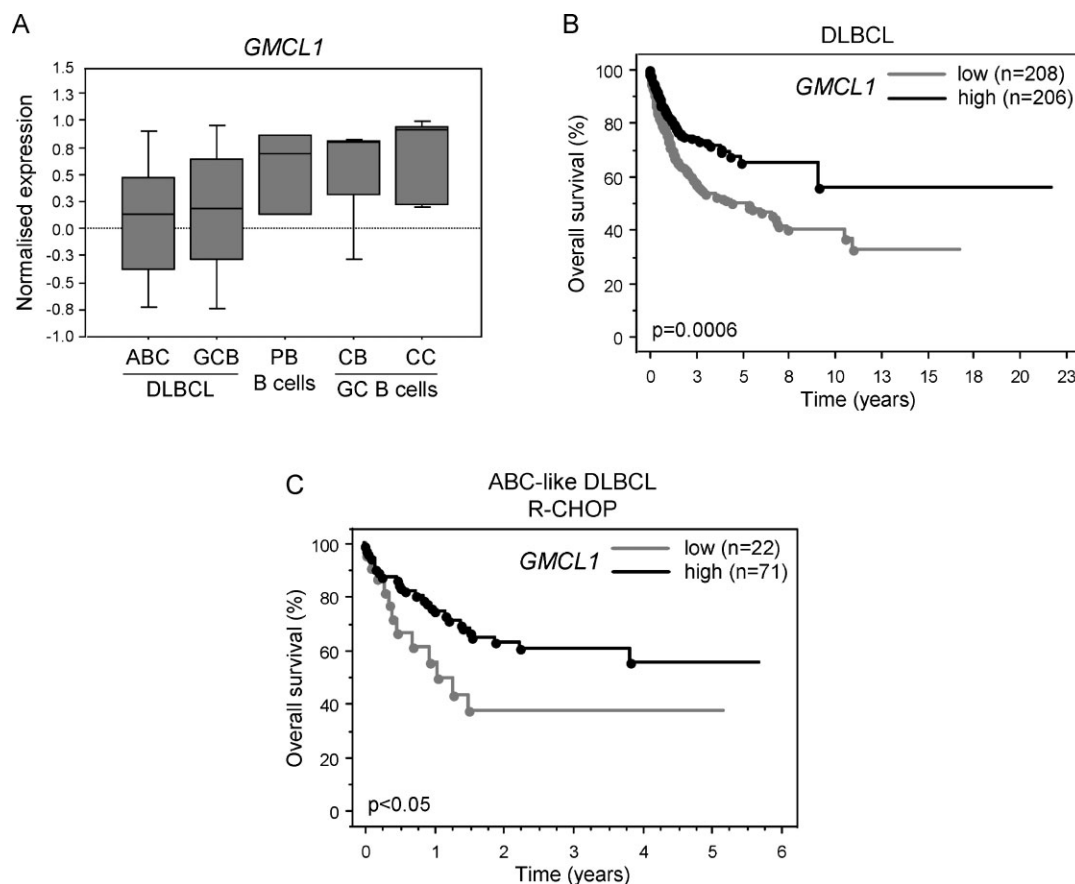


Figure 5. *GMCL1* mRNA expression correlates with prognosis in DLBCL.

(A) *GMCL1* expression levels in DLBCL (Diffuse Large B Cell Lymphoma) and normal B cells; Data from GSE 10846 (Lenz et al, 2008); 414 DLBCL patients: 181 treated by CHOP; 233 treated by R-CHOP. GCB, germinal centre B cell like; ABC, activated B cell like; PB, peripheral blood; CB, centroblasts; CC, centrocytes.

(B) Kaplan–Meier plots showing overall survival in DLBCL ($n = 414$).

(C) Kaplan–Meier plots showing overall survival in high risk DLBCL ($n = 93$).

Patient subgroups defined by expression compared to median normalized *GMCL1* mRNA levels.

with blocking reagent during 15 min without agitation. DNA methylation was detected using an anti-5-methylcytosine antibody serum (a gift from A. Niveleau) at a 1/5 dilution in modified PBS for 1 h at 37°C. Following two 5 min washes anti-5-methylcytosine signals were revealed with an FITC-labelled secondary antibody (DAKO) for 45 min at 37°C. Non-specific signal was removed by two washes in 1× PBS. The slides were air dried and mounted in an anti-fade/DAPI (4',6-diamino-2-phenylindole 0.5 mg/ml) solution, for microscope analysis. Analysis was performed on a Zeiss epifluorescence microscope (lamp HB 100W) equipped with a CCD camera under a 100× oil immersion objective. A total of 30 metaphases were analysed. This assay does not detect methylation at centromeres, in our hands.

ChIP on native and cross-linked chromatin

ChIP on native and cross-linked chromatin was performed as previously described (du Chene et al, 2007; Govin et al, 2007; Umlauf et al, 2004). All Q-ChIP assays were performed on at least three independent chromatin preparations. Details of the antibodies used are given in Table SII of the Supporting Information. For Q-PCR analyses of

immunoprecipitated chromatin fractions at sequences of interest, a SYBR Green PCR kit (Applied Biosystems) was used. Q-PCR was performed in duplicate on 25 ng of immunoprecipitated DNA or DNA from input chromatin fractions using the following conditions; 40 cycles at 95°C for 15 s, 60°C for 1 min. Primers pairs are listed in Table SIII of the Supporting Information. Q-PCR data obtained on immunoprecipitated fractions were normalized to input chromatin ($IP/Input = 2^{\Delta Ct} = 2^{[Ct(IP) - Ct(Input)]}$). Background precipitation was evaluated with a mock IP.

FISH to metaphase chromosomes and to interphase 2D and 3D nuclei

FISH to metaphase chromosomes for translocation breakpoint mapping purposes was performed as described (Lefebvre et al, 2007). Interphase FISH experiments (2D or 3D-FISH) were performed as described (Barki-Celli et al, 2005). Briefly, 16 h prior to harvesting, cells were diluted to 0.5×10^6 /ml in RPMI medium. Cells were harvested and resuspended at a concentration of 2.5×10^6 /2 ml of nuclei buffer (5 mM HEPES, 50 mM KCL, 10 mM $MgSO_4$, 0.05% Tween-20 pH 8) with 30 μ l of RNase (10 mg/ml), permeabilized and fixed, as

The paper explained

PROBLEM:

Numerous cancers present chromosomal translocations that can be broadly divided into those that mediate proto-oncogene activation by position effect and those that generate oncogenic fusion products. Chromosomal translocations that target repetitive sequences of the human genome are described as well, although their pathogenic consequences remain unclear. Rearrangements affecting the pericentric heterochromatic band, 1q12 are frequently observed in both haematological and solid tumours and this study set out to assess the impact of 1q12 satellite DNA anomalies on epigenome organization and function in B-cell tumours.

RESULTS:

This study shows that chromosomal translocations which target constitutive heterochromatin derived from human chromosome 1 (1q12) constitute a novel class of chromosomal anomaly that

mediates extensive, long range epigenome deregulations. They provoke the formation of aHCF in lymphoma B cells with consequent intrachromosomal pairing between the translocated satellite II DNA and centromeric regions. aHCF were found at the nuclear periphery and are associated to abnormal spatial positioning and expression of *GMCL1*. *GMCL1* is a candidate tumour suppressor gene localized to 2p and appears to have prognostic value in B cell lymphoma. 2p sequences adjacent to aHCF show increased levels of heterochromatin 'marks' such as trimethylation of lysines 9 and 20 on histones H3 and H4, respectively, and binding by the heterochromatin protein, HP1.

IMPACT:

We propose that 1q12 rearrangements, which are frequently encountered in a broad spectrum of human cancers, represent a new paradigm for long-range epigenetic deregulations in cancer.

described (Ferguson & Ward, 1992). The released nuclei were collected by centrifugation and washed three times in 1× PBS. Nuclei (50,000–100,000) were then cytocentrifuged onto Vectabond-treated glass slides (Vector Laboratories). These slides were stored for a maximum of 3 weeks prior to use in 2D or 3D immuno-FISH or 2D-FISH experiments. The 1q12 heterochromatin region was detected using the pUC1.77 probe, chromosome 1 and chromosome 2 centromeres using commercial probes (Vysis), as described (Le Baccon et al, 2001). Locus-specific FISH was performed with BACs selected from the Sanger Centre Ensembl or UCSC genome browsers. 2p gene and BAC probes used in the study were as follows: RP11-564H1 and RP11-321C18 (*EXOC6B*), RP11-7707 and RP11-401N16 (*GMCL1*). For FISH, BACs were directly labelled with cyanine 5-modified nucleotides by using a commercial nick translation kit (Vysis), according to the manufacturer's instructions. For repeat sequence probes, 50 ng of labelled DNA was used for FISH while for BAC probes 200 ng was used. Prior to FISH, slides were rinsed twice in 2× SSC, then permeabilized (Triton X-100/Saponine 0.5%/1× PBS) twice for 10 min to allow penetration of the probe. Non-specific sites were blocked in 3% BSA/2× SSC for 30 min at 37°C. Slides were then rinsed in 2× SSC and incubated for 10 min in 50% formamide/2× SSC. FISH was performed as previously described with the following modifications; nuclei were preincubated in hybridization buffer for 30 min prior to co-denaturation of probe and target, for 5 min at 86°C. The addition of COT-1 DNA was performed to reduce background hybridization. Washes were performed, as described, to remove non-specific signal (Barki-Celli et al, 2005; Lefebvre et al, 2007).

FISH Image analysis

For translocation breakpoint mapping purposes, FISH signals were captured in two-dimensional samples on a Zeiss Axioskop epifluorescence camera equipped with triple band pass filter by cooled CCD

camera. For 3D-immuno-FISH and analysis of radial nuclear distributions of 1q12 domains, three-dimensional analysis and image deconvolution was performed as described (Barki-Celli et al, 2005). To calculate the distance between two probes in 2D, the hybridization signals were manually segmented and the XY coordinates of the centroid of each were determined. 3D images of labelled cell nuclei were acquired in a wide-field epifluorescence mode using an Axiovert200M microscope (Zeiss) equipped with a 63×/1.4 plan-apochromat oil immersion lens, a piezoelectric stage and a cooled CCD camera CoolSnap HQ2 (Roper). The 15 μm stacks were registered in four colours with an axial step of 0.2 μm and processed by iterative deconvolution with the measured PSFs and Meinel algorithm (MetaMorph, Roper Scientific). The resulting images were then thresholded and the 3D distances between the barycentres of FISH signals were quantified using the 4D-Viewer software package (Roper). Statistical analysis was performed with the Statview package using the Kolmogorov–Smirnov (KS) and Kruskal–Wallis (KW) tests of significance, as indicated (Barki-Celli et al, 2005).

Array-CGH

Genome-wide analysis of DNA copy number changes in CH1 cells was performed using a high resolution microarray containing 240,000 probes (Human genome CGH array 244K, Agilent), as described (Jardin et al, 2009). Digestion was performed as recommended by the manufacturer of the arrays. Tumour DNA was labelled with cyanine-5 (Cy5) and reference DNA (pooled normal DNA, Promega, Madison, WI) was labelled with cyanine-3 (Cy3). Microarray image analysis and extraction were performed with Agilent Feature Extraction 9.5.3.1 software. Data analysis was performed with Agilent CGH-Analytics 3.4.27 software. Classification as gain or loss was based on the ADM-2 algorithm as implemented in CGH-analytics (threshold 6) and a visual inspection of the log₂ ratios. Data sets were reviewed for frequently

affected chromosomal sites of physiological copy number variations (CNV), using comparison with the genomic variants database (<http://projects.tcag.ca/variation/>).

Q-RT-PCR analysis

Total RNA was extracted from cell lines and purified normal and tumour B cells by TRIzol reagent (Invitrogen Life Technologies), quality controlled by using the Agilent Bioanalyzer system, and quantified by NanoDrop (Thermo Scientific) before being reverse transcribed using the SuperScript[®] III First-Strand Synthesis SuperMix for qRT-PCR (Invitrogen Life Technologies), according to the manufacturer's instructions. Q-PCR was performed using SYBR[®] Green PCR master mix (Applied Biosystems) and primers shown in Table SIII of the Supporting Information, according to the manufacturer's instructions. Quantification was achieved against standard curves run in parallel in each PCR assay for each target. The U6 gene was used as a control gene for normalization of gene expression data. Q-PCR was performed on a MX3000P (Stratagene) machine.

Affymetrix gene expression profiling

Biotinylated cRNA prepared from total RNA, as described above, was amplified with double *in vitro* transcription and hybridized to the Affymetrix HG U133 Plus 2.0 microarrays, according to the manufacturer's instructions (Affymetrix, Santa Clara, CA, USA). Fluorescence intensities were quantified and analysed using the GCOS 1.2 software (Affymetrix). Gene expression data were normalized with the MAS5 algorithm by scaling each array to a target value of 100 using the *global scaling* method. The raw gene-expression data are available at www.ncbi.nlm.nih.gov/geo (GSE20666). Statistical analysis was performed using the GeneSpring software package (Agilent). For assessment of gene expression changes at the 1q12/2p breakpoint sequence in CH1 cells, a moving average approach with 500 kb windows was used to compare gene expression values to similar sized regions of equal copy number in the rest of the genome (4833 probes). Gene expression and survival analysis in the LLMPP data set (Lenz et al, 2008) was performed using gene expression data that had been normalized by RMA using Gene Spring software, followed by statistical analysis in the Statview package, by using the Logrank Mantel–Cox test and median normalized *GMCL1* expression as a threshold.

Author contributions

AF performed and was responsible for analysis of the main experiments of the article, including 3D FISH, Q-ChIP, and Affymetrix gene chip data, and co-wrote the paper. AMLF performed Q-RT-PCR, immuno-FISH, analysed gene expression and ChIP data and contributed to the writing of the paper. CL analysed 3D FISH data and with DL performed cytogenetic analyses, provided patient samples and expert advice. SD performed ChIP and 3D-FISH image analyses. LB, KA, SH and AuG performed Q-ChIP assays and cell culture. JBR performed normal and lymphoma B cell purification with expert advice from AL and TB. SC performed cell culture. AD performed survival analysis under the supervision of SR, RG and MC. MF JdV and SR performed Affymetrix gene expression analyses. FdF performed DNA methylation analyses. JPK and MF performed aCGH analyses. AIG performed 3D FISH analysis

with expert advice from YU. KD provided training in ChIP. CV, DL, SK and RF provided expert guidance throughout the study and contributed to the writing of the manuscript. MC proposed the concept, coordinated the study, supervised the design and analyses of the experiments and wrote the paper.

Acknowledgements

We thank Stefan Dimitrov and Rosemary Kiernan for invaluable assistance and advice with cross-linked ChIP analyses. We acknowledge Prof. Jean-Jacques Sotto, Prof. Jean-Yves Cahn, Prof. Eric Gilson and Prof. Jean Feunteun and members of the ARAMIS association for their encouragement of this work. Funding was from the Fondation de France, the Institut National du Cancer (EpiPro network, the programme 'Développement de plateformes hospitalières de génétique moléculaire des cancers', the P.A.I.R 'Mantle Cell Lymphoma network' and the INCa-DHOS translational research programme 'CT-Lymph') and the Association pour la Recherche sur le Cancer (ARECA programme). Additional funding was obtained from the Région Rhone-Alpes programme 'Thématique prioritaire—Cancer', the canceropôle CLARA (EpiMed), the Ligue Nationale Contre le Cancer (LNCC)—Comités de l'Isère/Savoie, the Délégation Régionale de la Recherche Clinique—CHU de Grenoble, the French GOELAMS clinical trials group and the ARAMIS association. AD and JBR have been recruited through the INCa-DHOS 'CT-Lymph' program. AF has been the recipient of doctoral funding from the Ministère de l'Enseignement Supérieur et de la Recherche, the Association pour la Recherche sur le Cancer (ARC) and the Société Française d'Hématologie (SFH); AMLF of post-doctoral funding from the ARC-ARECA network 'epigenetic profiling in breast and haematological tumours'; LB of doctoral funding from the Ministère de l'Enseignement Supérieur et de la Recherche and the LNCC; MC of a Contrat d'Interface INSERM/Grenoble University Hospital Centre (2006–2011). Affymetrix microarrays were processed in the Microarray Core Facility of the Institute of Research on Biotherapy, CHRU-INSERM-UM1 Montpellier, <http://irb.chu-montpellier.fr/>

Supporting information is available at EMBO Molecular Medicine online.

The authors declare no competing financial interests.

For more information

Oncomine transcriptome database:
<http://www.oncomine.org>

References

- Alizadeh AA, Eisen MB, Davis RE, Ma C, Lossos IS, Rosenwald A, Boldrick JC, Sabet H, Tran T, Yu X, et al (2000) Distinct types of diffuse large B-cell lymphoma identified by gene expression profiling. *Nature* 403: 503–511
- Barki-Celli L, Lefebvre C, Le Baccon P, Nadeau G, Bonnefoix T, Usson Y, Vourc'h C, Khochbin S, Leroux D, Callanan M (2005) Differences in nuclear

- positioning of 1q12 pericentric heterochromatin in normal and tumor B lymphocytes with 1q rearrangements. *Genes Chromosomes Cancer* 43: 339-349
- Bernstein E, Allis CD (2005) RNA meets chromatin. *Genes Dev* 19: 1635-1655
- Brown KE, Guest SS, Smale ST, Hahn K, Merckenschlager M, Fisher AG (1997) Association of transcriptionally silent genes with Ikaros complexes at centromeric heterochromatin. *Cell* 91: 845-854
- Brown KE, Baxter J, Graf D, Merckenschlager M, Fisher AG (1999) Dynamic repositioning of genes in the nucleus of lymphocytes preparing for cell division. *Mol Cell* 3: 207-217
- Busson-Le Coniat M, Salomon-Nguyen F, Dastugue N, Maarek O, Lafage-Pochitaloff M, Mozziconacci MJ, Baranger L, Brizard F, Radford I, Jeanpierre M, et al (1999) Fluorescence in situ hybridization analysis of chromosome 1 abnormalities in hematopoietic disorders: rearrangements of DNA satellite II and new recurrent translocations. *Leukemia* 13: 1975-1981
- Callanan MB, Le Baccon P, Mossuz P, Duley S, Bastard C, Hamoudi R, Dyer MJ, Klobbeck G, Rimokh R, Sotto JJ, et al (2000) The IgG Fc receptor, FcγRIIB, is a target for deregulation by chromosomal translocation in malignant lymphoma. *Proc Natl Acad Sci USA* 97: 309-314
- Dernburg AF, Broman KW, Fung JC, Marshall WF, Phillips J, Agard DA, Sedat JW (1996) Perturbation of nuclear architecture by long-distance chromosome interactions. *Cell* 85: 745-759
- du Chene I, Basyuk E, Lin YL, Triboulet R, Knezevich A, Chable-Bessia C, Mettling C, Baillat V, Reynes J, Corbeau P, et al (2007) Suv39H1 and HP1γ are responsible for chromatin-mediated HIV-1 transcriptional silencing and post-integration latency. *EMBO J* 26: 424-435
- Feinberg AP, Ohlsson R, Henikoff S (2006) The epigenetic progenitor origin of human cancer. *Nat Rev Genet* 7: 21-33
- Ferguson M, Ward DC (1992) Cell cycle dependent chromosomal movement in pre-mitotic human T-lymphocyte nuclei. *Chromosoma* 101: 557-565
- Finlan LE, Sproul D, Thomson I, Boyle S, Kerr E, Perry P, Ylstra B, Chubb JR, Bickmore WA (2008) Recruitment to the nuclear periphery can alter expression of genes in human cells. *PLoS Genet* 4: e1000039
- Fournier A, Florin A, Lefebvre C, Solly F, Leroux D, Callanan MB (2007) Genetics and epigenetics of 1q rearrangements in hematological malignancies. *Cytogenet Genome Res* 118: 320-327
- Fraga MF, Ballestar E, Villar-Garea A, Boix-Chornet M, Espada J, Schotta G, Bonaldi T, Haydon C, Ropero S, Petrie K, et al (2005) Loss of acetylation at Lys16 and trimethylation at Lys20 of histone H4 is a common hallmark of human cancer. *Nat Genet* 37: 391-400
- Govin J, Escoffier E, Rousseaux S, Kuhn L, Ferro M, Thevenon J, Catena R, Davidson I, Garin J, Khochbin S, et al (2007) Pericentric heterochromatin reprogramming by new histone variants during mouse spermiogenesis. *J Cell Biol* 176: 283-294
- Grewal SI, Jia S (2007) Heterochromatin revisited. *Nat Rev Genet* 8: 35-46
- Grogan JL, Mohrs M, Harmon B, Lacy DA, Sedat JW, Locksley RM (2001) Early transcription and silencing of cytokine genes underlie polarization of T helper cell subsets. *Immunity* 14: 205-215
- Hiratani I, Gilbert DM (2009) Replication timing as an epigenetic mark. *Epigenetics* 4: 93-97
- Itoyama T, Nanjungud G, Chen W, Dyomin VG, Teruya-Feldstein J, Jhanwar SC, Zelenetz AD, Chaganti RS (2002) Molecular cytogenetic analysis of genomic instability at the 1q12-22 chromosomal site in B-cell non-Hodgkin lymphoma. *Genes Chromosomes Cancer* 35: 318-328
- Jardin F, Callanan M, Penther D, Ruminy P, Troussard X, Kerckaert JP, Figeac M, Parmentier F, Rainville V, Vaida I, et al (2009) Recurrent genomic aberrations combined with deletions of various tumour suppressor genes may deregulate the G1/S transition in CD4+CD56+ haematodermic neoplasms and contribute to the aggressiveness of the disease. *Leukemia* 23: 698-707
- Krouwels IM, Wiesmeijer K, Abraham TE, Molenaar C, Verwoerd NP, Tanke HJ, Dirks RW (2005) A glue for heterochromatin maintenance: stable SUV39H1 binding to heterochromatin is reinforced by the SET domain. *J Cell Biol* 170: 537-549
- Kumaran RI, Spector DL (2008) A genetic locus targeted to the nuclear periphery in living cells maintains its transcriptional competence. *J Cell Biol* 180: 51-65
- Lajmanovich A, Ribeyron JB, Florin A, Fournier A, Pasquier MA, Duley S, Chauvet M, Plumas J, Bonnefoix T, Gressin R, et al (2009) Identification, characterisation and regulation by CD40 activation of novel CD95 splice variants in CD95-apoptosis-resistant, human, B-cell non-Hodgkin's lymphoma. *Exp Cell Res* 315: 3281-3293
- Le Baccon P, Leroux D, Dascalescu C, Duley S, Marais D, Esmenjaud E, Sotto JJ, Callanan M (2001) Novel evidence of a role for chromosome 1 pericentric heterochromatin in the pathogenesis of B-cell lymphoma and multiple myeloma. *Genes Chromosomes Cancer* 32: 250-264
- Lefebvre C, Fabre B, Vettier C, Rabin L, Florin A, Wang J, Gressin R, Jacob MC, Callanan M, Leroux D (2007) Composite splenic marginal zone lymphoma and mantle cell lymphoma arising from 2 independent B-cell clones. *Hum Pathol* 38: 660-667, Epub 2006 Nov 28
- Lenz G, Wright G, Dave SS, Xiao W, Powell J, Zhao H, Xu W, Tan B, Goldschmidt N, Iqbal J, et al (2008) Stromal gene signatures in large-B-cell lymphomas. *N Engl J Med* 359: 2313-2323
- Masuhara M, Nagao K, Nishikawa M, Kimura T, Nakano T (2003) Enhanced degradation of MDM2 by a nuclear envelope component, mouse germ cell-less. *Biochem Biophys Res Commun* 308: 927-932
- Popova BC, Tada T, Takagi N, Brockdorff N, Nesterova TB (2006) Attenuated spread of X-inactivation in an X autosome translocation. *Proc Natl Acad Sci USA* 103: 7706-7711
- Popova BC, Tada T, Takagi N, Brockdorff N, Nesterova TB (2006) Attenuated spread of X-inactivation in an X autosome translocation. *Proc Natl Acad Sci USA* 103: 7706-7711
- Rabbitts TH (2009) Commonality but diversity in cancer gene fusions. *Cell* 137: 391-395
- Reddy KL, Zullo JM, Bertolino E, Singh H (2008) Transcriptional repression mediated by repositioning of genes to the nuclear lamina. *Nature* 452: 243-247
- Sawyer JR, Tricot G, Mattox S, Jagannath S, Barlogie B (1998) Jumping translocations of chromosome 1q in multiple myeloma: evidence for a mechanism involving decondensation of pericentromeric heterochromatin. *Blood* 91: 1732-1741
- Sawyer JR, Tricot G, Lukacs JL, Binz RL, Tian E, Barlogie B, Shaughnessy Jr J (2005) Genomic instability in multiple myeloma: evidence for jumping segmental duplications of chromosome arm 1q. *Genes Chromosomes Cancer* 42: 95-106
- Souza PP, Volkel P, Trinel D, Vandamme J, Rosnoble C, Heliot L, Angrand PO (2009) The histone methyltransferase SUV420H2 and Heterochromatin Proteins HP1 interact but show different dynamic behaviours. *BMC Cell Biol* 10: 41
- Su RC, Brown KE, Saaber S, Fisher AG, Merckenschlager M, Smale ST (2004) Dynamic assembly of silent chromatin during thymocyte maturation. *Nat Genet* 36: 502-506
- Takizawa T, Meaburn KJ, Misteli T (2008) The meaning of gene positioning. *Cell* 135: 9-13
- Umlauf D, Goto Y, Cao R, Cerqueira F, Wagschal A, Zhang Y, Feil R (2004) Imprinting along the Kcnq1 domain on mouse chromosome 7 involves repressive histone methylation and recruitment of Polycomb group complexes. *Nat Genet* 36: 1296-1300
- Vogel MJ, Pagie L, Talhout W, Nieuwland M, Kerkhoven RM, van Steensel B (2009) High-resolution mapping of heterochromatin redistribution in a *Drosophila* position-effect variegation model. *Epigenetics Chromatin* 2: 1